

Supporting Information

Theoretical investigation of electrocatalytic activity of oxygen evolution/reduction reactions of ruthenium polyphthalocyanine axially modified with aliphatic thiols

Guilin Wang^{a,b}, Xiaoqin Feng^a, Rongrong Ren^a, Yuxin Wang^a, Jie Meng^a, Jianfeng Jia^{a,*}

^aKey Laboratory of Magnetic Molecules and Magnetic Information Materials (Ministry of Education), School of Chemistry and Material Science, Shanxi Normal University, Taiyuan 030031, China

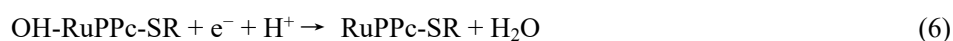
^bDepartment of Physics and Electronic Engineering, Yuncheng University, Yuncheng 044000, China

E-mail: jjajf@dns.sxnu.edu.cn

Table S1. The lattice parameters (in Å or °) of cell of RuPPc and RuPPc-SR. Average bond length of Ru-N bond ($b_{\text{Ru-N}}$, in Å) of RuPPc and RuPPc-SR.

Structure	Lattice parameter					$b_{\text{Ru-N}}$ (Å)
	a (Å)	b (Å)	α (°)	β (°)	γ (°)	
RuPPc	10.73	10.73	90.00°	90.00°	90.00°	1.99
RuPPc-SCH ₃	10.74	10.75	90.39°	88.39°	90.15°	2.00
RuPPc-SC ₂ H ₅	10.73	10.75	90.64°	89.21°	90.04°	2.01
RuPPc-SC ₃ H ₇	10.74	10.74	93.45°	90.92°	89.90°	2.00
RuPPc-SC ₄ H ₉	10.76	10.72	89.38°	91.22°	90.04°	2.00
RuPPc-SC ₅ H ₁₁	10.73	10.73	90.45°	92.41°	90.02°	2.00
RuPPc-SC ₆ H ₁₃	10.73	10.73	90.90°	95.00°	90.00°	2.00

The Pourbaix plots can be used to analyze the stability of different phases of catalyst under different H⁺ concentration and potential conditions.^{1,2} We constructed surface Pourbaix plots using the ground state energies, ZPE, and entropic contributions for RuPPc/RuPPc-SR, H-RuPPc/H-RuPPc-SR, and HO-RuPPc/HO-RuPPc-SR systems at standard conditions and at 298 K. Considered surface processes² include:



According to the above electrode reaction equations (1)-(6), the following Nernst equations can be established:

$$E(\text{Ru}^{2+}/\text{RuPPc}) = E^0(\text{Ru}^{2+}/\text{RuPPc}) - 0.0592/2 \times \log a(\text{Ru}^{2+}) \quad (7)$$

$$E(\text{Ru}^{3+}/\text{RuPPc-SR}) = E^0(\text{Ru}^{3+}/\text{RuPPc-SR}) - 0.0592/3 \times \log a(\text{Ru}^{3+}) \quad (8)$$

$$E(\text{RuPPc}/\text{H-RuPPc}) = E^0(\text{RuPPc}/\text{H-RuPPc}) - 0.0592 \times \text{pH} \quad (9)$$

$$E(\text{RuPPc-SR}/\text{H-RuPPc-SR}) = E^0(\text{RuPPc-SR}/\text{H-RuPPc-SR}) - 0.0592 \times \text{pH} \quad (10)$$

$$E(\text{HO-RuPPc}/\text{RuPPc}) = E^0(\text{HO-RuPPc}/\text{RuPPc}) - 0.0592 \times \text{pH} \quad (11)$$

$$E(\text{HO-RuPPc-SR}/\text{RuPPc-SR}) = E^0(\text{HO-RuPPc-SR}/\text{RuPPc-SR}) - 0.0592 \times \text{pH} \quad (12)$$

Where E^0 is the standard equilibrium potential. The equilibrium potential (E) in the pH range of 0 ~ 14 is calculated by equations (7)-(12). The activity (a) of Ru²⁺ and Ru³⁺ ions were taken to be $1 \times 10^{-8} \text{ mol dm}^{-3}$.^{2,3} The calculated standard potentials for reactions at standard conditions, 298 K, pH = 0 are summarized in Table S2. Pourbaix plots were constructed for the RuPPc and RuPPc-SC₄H₉ as shown in Fig. 4, and for the other RuPPc-SR are shown in Fig. S4.

Table S2. Calculated standard potentials for reactions based on the equations (1) to (6), at standard conditions, 298 K, pH = 0.

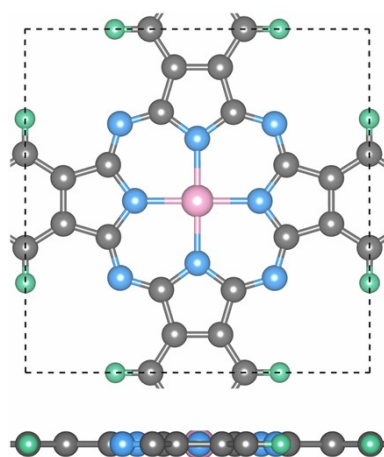
Structure	z	$E^\theta(\text{Ru}^{2+}/\text{RuPPc})/$ $E^\theta(\text{Ru}^{3+}/\text{RuPPc-SR})$	$E^\theta(\text{RuPPc}/\text{H-RuPPc})/$ $E^\theta(\text{RuPPc-SR}/\text{H-RuPPc-SR})$	$E^\theta(\text{HO-RuPPc}/\text{RuPPc})/$ $E^\theta(\text{HO-RuPPc-SR}/\text{RuPPc-SR})$
RuPPc	2	6.456	0.437	0.306
RuPPc-SCH ₃	3	3.180	-0.761	0.991
RuPPc-SC ₂ H ₅	3	2.111	-0.758	0.994
RuPPc-SC ₃ H ₇	3	2.106	-0.710	0.845
RuPPc-SC ₄ H ₉	3	2.114	-0.830	0.993
RuPPc-SC ₅ H ₁₁	3	2.113	-0.784	0.844
RuPPc-SC ₆ H ₁₃	3	2.129	-1.152	0.844

Table S3. The adsorption free energies (unit: eV) of intermediates of ORR/OER of RuPPc and RuPPc-SR, which were calculated using the PBE and the PBE + U.

Structure	PBE					PBE+U				
	$\Delta G_{\text{H}}^{*\text{OO}}$ (eV)	ΔG_{O}^{*} (eV)	ΔG_{OH}^{*} (eV)	η^{ORR} (V)	η^{OER} (V)	$\Delta G_{\text{OOH}}^{*}$ (eV)	ΔG_{O}^{*} (eV)	ΔG_{OH}^{*} (eV)	η^{ORR} (V)	η^{OER} (V)
RuPPc	3.183	1.045	0.270	0.960	0.903	3.592	1.301	0.547	0.683	1.061
RuPPc-SCH ₃	4.007	2.052	0.977	0.309	0.721	3.984	2.247	0.957	0.294	0.508
RuPPc-SC ₂ H ₅	3.760	2.091	0.863	0.367	0.435	3.918	2.277	0.910	0.320	0.411
RuPPc-SC ₃ H ₇	3.710	2.060	0.835	0.395	0.416	3.859	2.256	0.860	0.370	0.374
RuPPc-SC ₄ H ₉	3.789	2.119	0.993	0.237	0.436	3.860	2.294	0.997	0.233	0.336
RuPPc-SC ₅ H ₁₁	3.981	2.067	0.844	0.386	0.680	4.034	2.257	0.964	0.344	0.547
RuPPc-SC ₆ H ₁₃	4.001	2.064	0.846	0.384	0.703	4.043	2.256	0.965	0.353	0.558

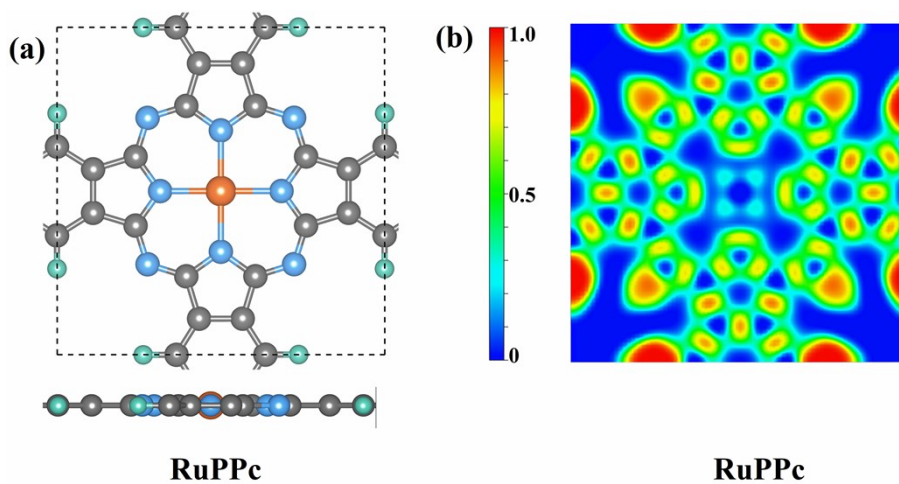
Table S4. Q_{Ru} (unit: |e|), Q_{N} (unit: |e|), and Q_{SR} (unit: |e|) denote the Bader charge of the Ru atom, the four N atoms closest to the Ru atom and the aliphatic thiol groups in the RuPPc and RuPPc-SR, respectively.

Structure	$Q_{\text{Ru}}(e)$	$Q_{\text{N4}}(e)$	$Q_{\text{SR}}(e)$
RuPPc	1.218	-4.537	---
RuPPc-SCH ₃	1.028	-4.518	-0.038
RuPPc-SC ₂ H ₅	1.147	-4.528	-0.037
RuPPc-SC ₃ H ₇	1.081	-4.535	-0.041
RuPPc-SC ₄ H ₉	1.015	-4.495	-0.017
RuPPc-SC ₅ H ₁₁	1.178	-4.438	-0.041
RuPPc-SC ₆ H ₁₃	1.115	-4.426	-0.042



FePPc

Fig.S1. The top and side view of the unit cell of FePPc.



RuPPc

RuPPc

Fig.S2. (a)The top and side view of the unit cell of RuPPc. The green, gray, blue, yellow, and orange balls are H, C, N, S, and Ru atoms, respectively. (b) The Electron localization functions (ELFs) of the top and side view of the RuPPc..

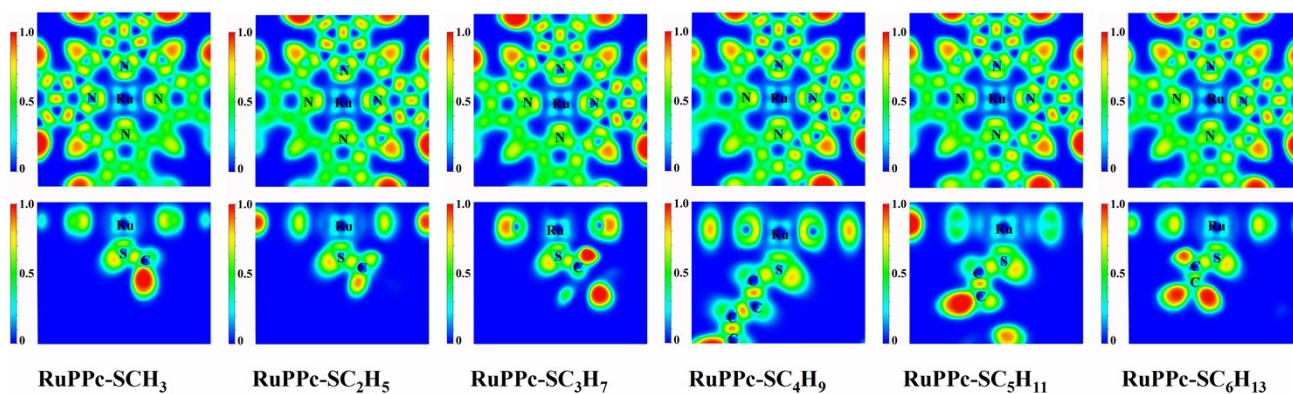


Fig.S3. The Electron localization functions (ELFs) of the top and side view of RuPPc-SR.

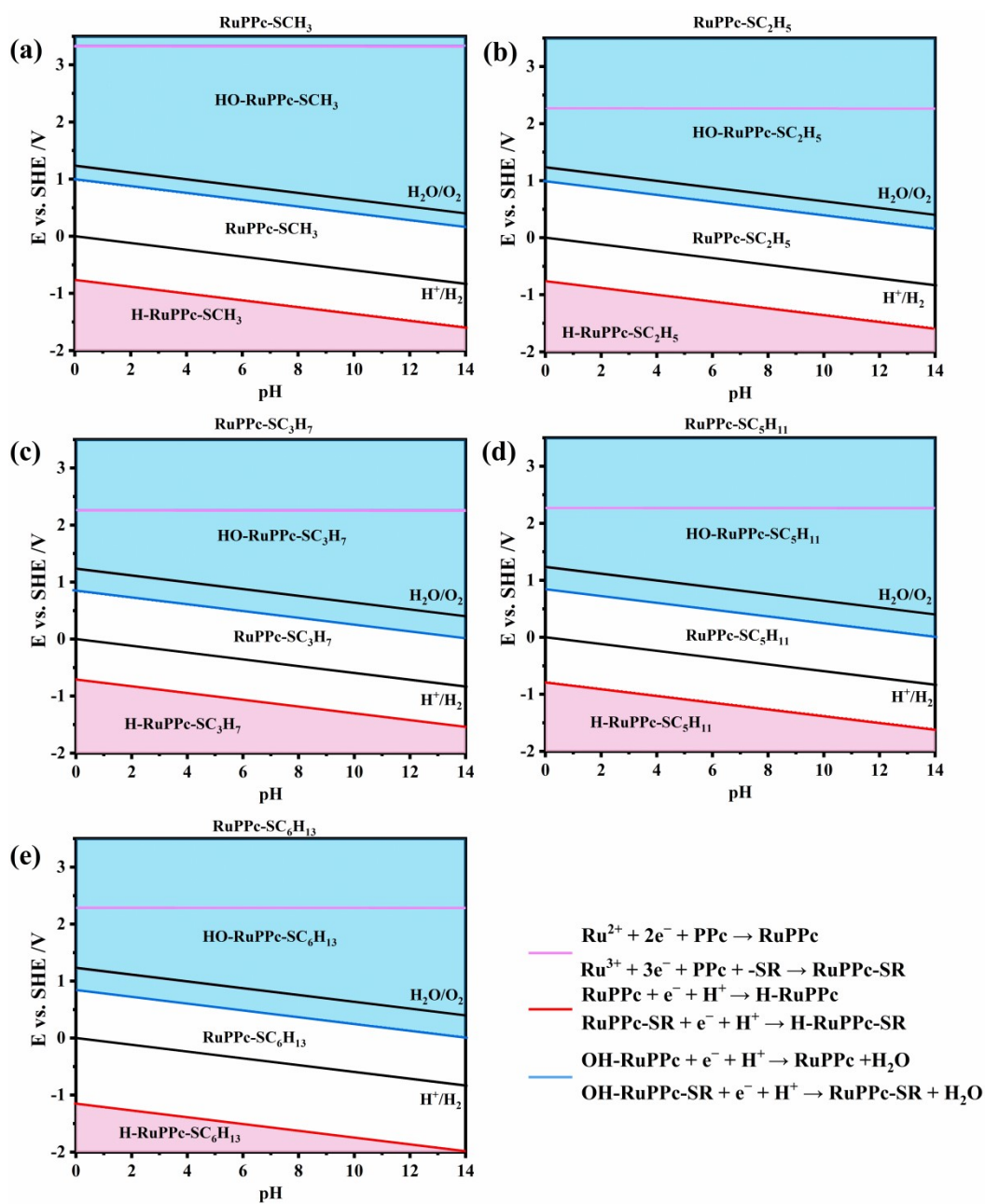


Fig.S4. Surface Pourbaix plots of RuPPc-SR. Thick black lines indicate the theoretical water stability region.

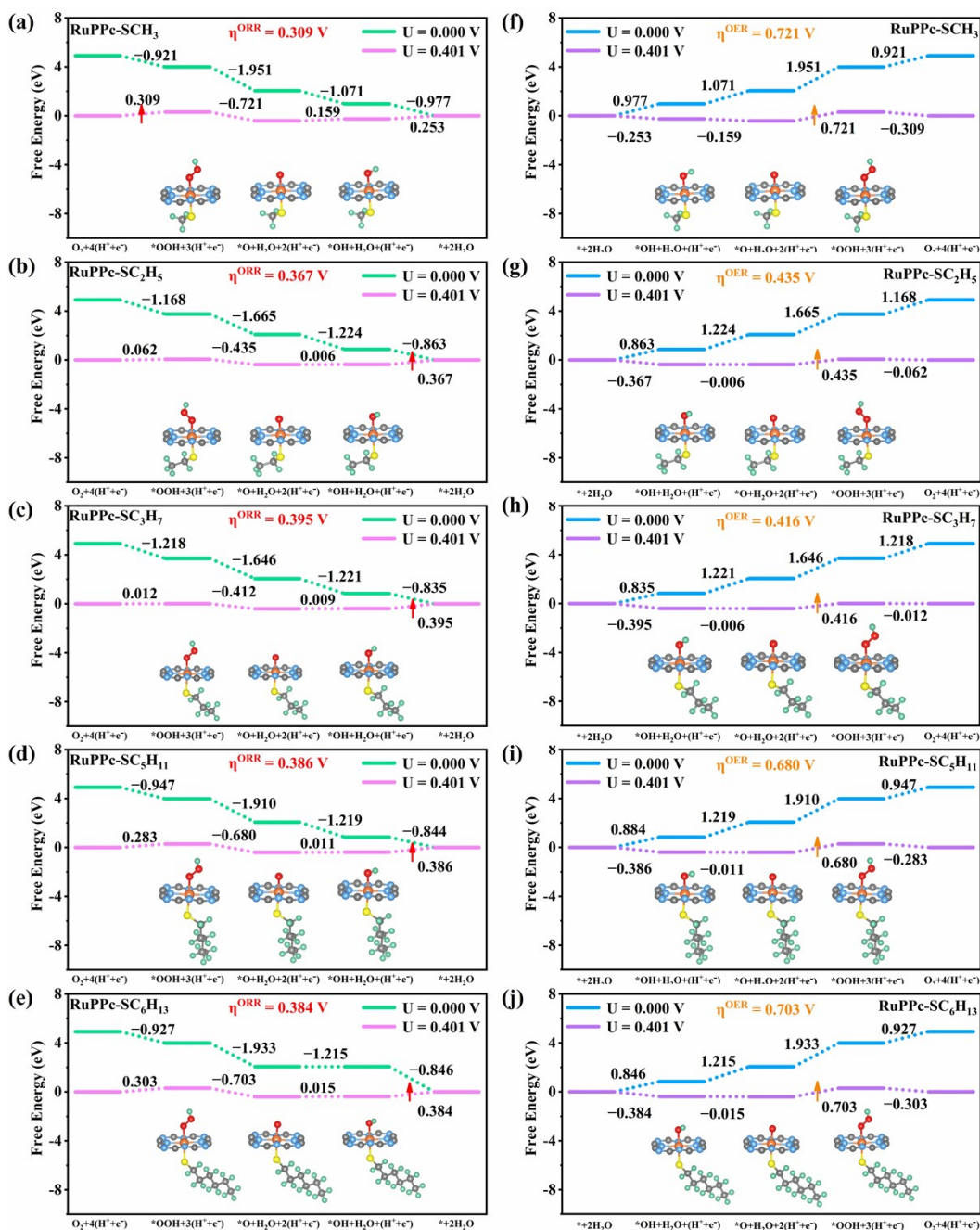


Fig. S5. (a)–(e) The ORR free energy diagrams of RuPPc-SR (SR = -SCH₃, -SC₂H₅, -SC₃H₇, -SC₅H₁₁, and -SC₆H₁₃) at $U = 0$ V, respectively. (f)–(j) The OER free energy diagrams of RuPPc and RuPPc-SR (SR = -SCH₃, -SC₂H₅, -SC₃H₇, -SC₅H₁₁, and -SC₆H₁₃) at $U = 0$ V, respectively. The red and orange upward arrows present the potential-determination step (PDS) of ORR and OER, respectively. The configurations of the reaction intermediates are also shown. The green, gray, blue, red, yellow, and orange balls are H, C, N, O, S, and Ru atoms, respectively.

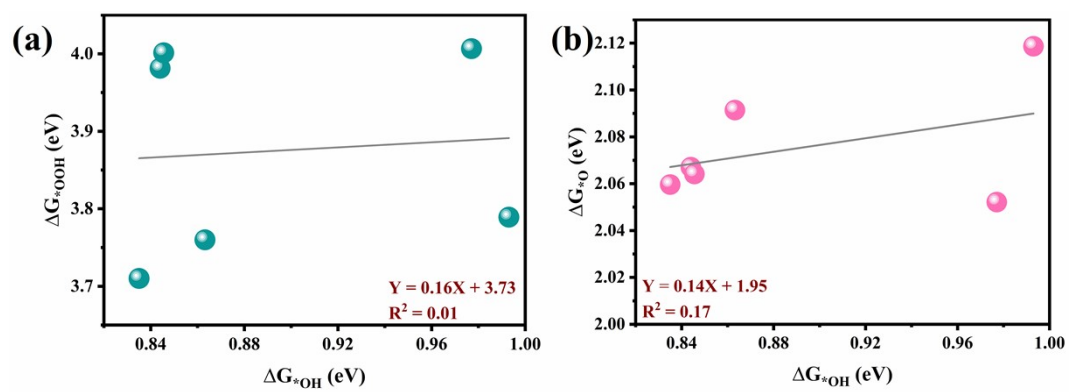


Fig. S6. (a) The fitting relationship of ΔG^*_{OOH} vs. ΔG^*_{OH} . (b) The fitting relationship of ΔG^*_O vs. ΔG^*_{OH} .

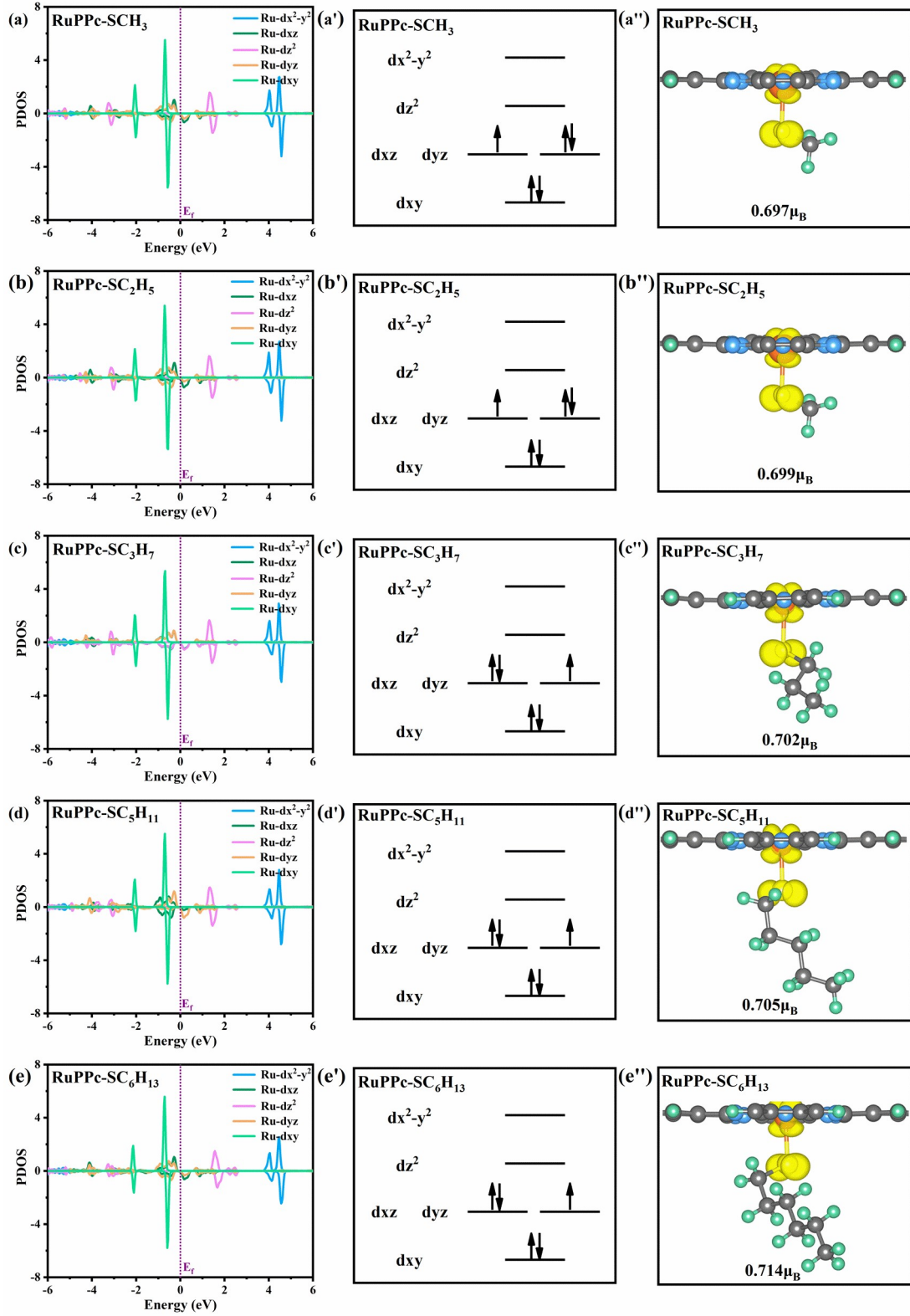


Fig.S7. (a)-(e) PDOS of RuPPc-SR. The vertical purple dotted line represents the Fermi level. (a')-(e') The electronic occupation of the five 4d orbitals of the Ru atoms RuPPc-SR. (a'')-(e'') Spin density distribution of RuPPc-SR. Yellow and turquoise iso-surfaces correspond to spin-up and spin-down density, respectively. The iso-surface levels are $0.002 \text{ e}/\text{\AA}^3$. M_{Ru} denotes the magnetic moment (unit: μ_{B}) of the Ru atoms in RuPPc-SR.

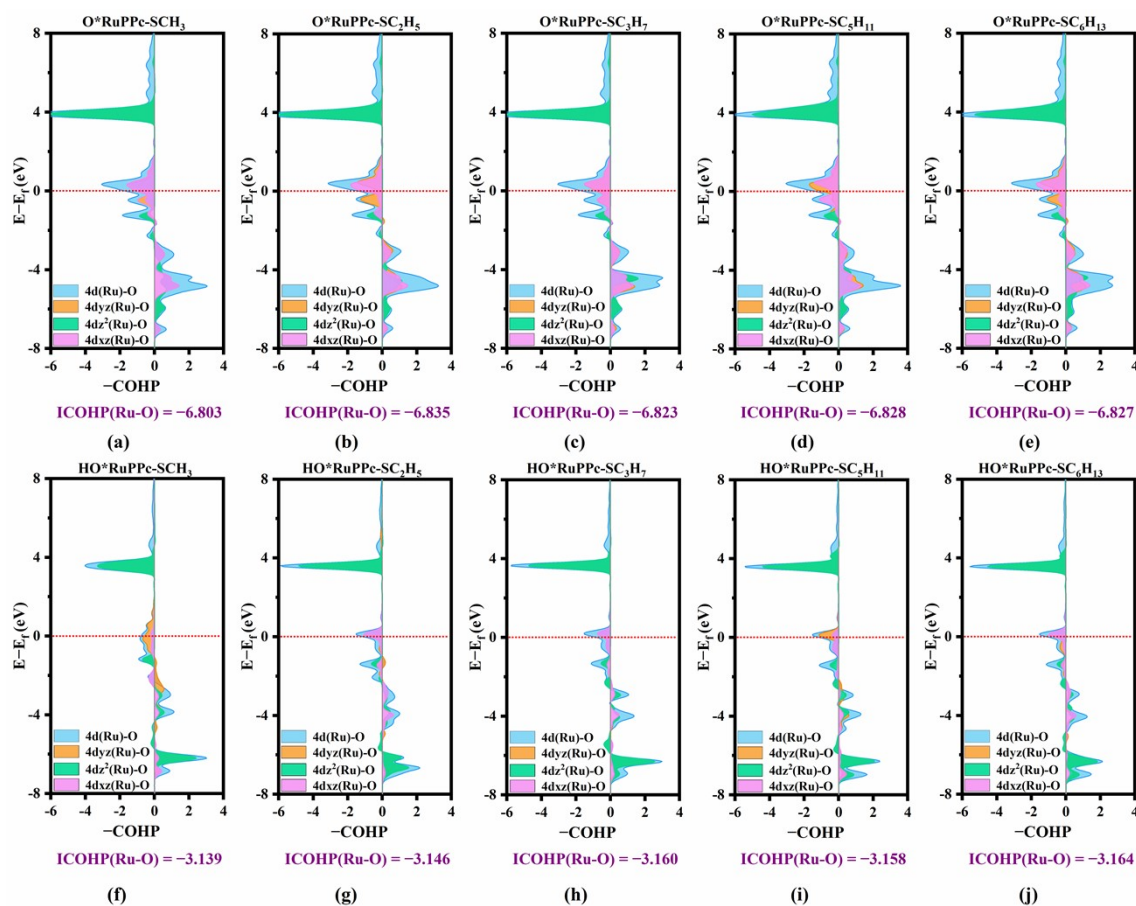


Fig. S8. (a)-(e) Crystal orbital Hamilton population (COHP) of the Ru-O bond in *O of RuPPc and RuPPc-SR, respectively. (f)-(j) Crystal orbital Hamilton population (COHP) of the Ru-O bond in *OH of RuPPc and RuPPc-SC₄H₉, respectively. ICOHP(Ru-O) is the integrated COHP of Ru-O bond. The horizontal red dotted line represents the E_f . The positive and the negative contributions denote the bonding states and anti-bonding states, respectively.

References:

1. A. K. Singh, L. Zhou, A. Shinde, S. K. Suram, J. H. Montoya, D. Winston, J. M. Gregoire and K. A. Persson, *Chemistry of Materials*, 2017, **29**, 10159-10167.
2. A. S. Dobrota, N. V. Skorodumova, S. V. Mentus and I. A. Pašti, *Electrochimica Acta*, 2022, **412**, 140155.
3. I. A. Pašti, A. Jovanović, A. S. Dobrota, S. V. Mentus, B. Johansson and N. V. Skorodumova, *Physical Chemistry Chemical Physics*, 2018, **20**, 858-865.